Investigation of Path-Loss Models for 5.8 GHz Radio Signals in Christopher Newport University's Luter Hall

David Cox

Adviser: Dr. Jonathan Backens

Christopher Newport University

Abstract:

This report accounts for a path loss study for a single tone-modulated signal at a carrier frequency of 5.8 GHz. The location for this study is set within the walls of Luter Hall at Christopher Newport University. In this environment, power attenuation during propagation is measured and compared to various path loss models. Software defined radios, running GNURadio, are used to both generated and receive the RF signals.

The project is composed of two experiments. The first experiment tests path loss through free space and in line of sight. The results of the experiment were compared to theoretical calculations derived from the Friis Transmission Equation. The second experiment tests path loss through a standard partition wall found between two labs in Luter Hall. The Partition Dependent model and measurements from Harris Semiconductors were used to create comparative data. The two data sets were then compared.

Error analysis was run between the measured path loss and the path loss models. All collected data was averaged. It is the average path loss that was compared to the path loss models. After comparison, the models were determined to be either valid predictors of path loss or not applicable. The ultimate goal of experiment is to produce the best model possible. Valid models will be adjusted to increase their accuracy. If a model is deemed not applicable, then a new, unique model will be devised and proposed. Although the models produced from this experiment are specific and unverified, they are the beginning steps to comprehensively model the propagation of a 5.8 GHz signal in Luter Hall.

Introduction:

Wireless communication systems are utilized in every aspect of life: recreation, business, healthcare, and industry. As the number of wireless devices increases, engineers are struggling to find enough frequency "real-estate" to accommodate all the devices. The solution is to develop deceives that operate at higher frequency bands. The cost of using higher frequencies is that the signal will become more susceptible to distortion. A wireless signal can become distorted in many different ways, but attenuation will be the primary focus of this experiment. In a physical sense, attenuation is the diminishing of the signal's power. Mathematically, a signal such as a sinusoid is being multiplied by a fractional coefficient, ex. (0.5)cos(x). The loss of power in a wireless communication system between transmitter and receiver is generally known as path loss. Path loss is a factor than cannot be estimated by a single equation. Instead, multiple equations for specific instances are needed to model the effect. This experiment will investigate path loss at a high radio frequency in Luter Hall at Christopher Newport University. The high frequency chosen to study is 5.8GHz. This frequency is significant because it is the next band to be utilized in the natural advancement in wireless communication.

Software defined radios (SDRs) will be used to measure the path loss of a simple signal being propagated from transmitter to receiver. GNURadio will provide the software used to define the radios and conduct measurements. The collected measurements will be used model path loss specifically in Luter Hall. In addition, the measurements will be compared to pre-existing models to determine if they are applicable at the frequency and location.

Path loss models vary to accommodate frequency, location, and possible obstructions. This experiment will focus on two specific scenarios. First, path loss through free space. In a large room in Luter Hall, the receiver and transmitter will be placed in line of sight of each other with no obstructions. The distance will be increased between the devices to measure the loss due to free space. The results will be compared to predictions made by the Friis Transmission equation (Bevelacqua). The second experiment will measure path loss through one standard, internal partition wall. The wall chosen divides two engineering labs. Using link budget, see Theory section of design report, an attenuation constant for the wall will be measured. The results will be compared to a preexisting, well accepted model for 2.4 GHz (Wi-Fi).

The experimental results should deliver valuable data for wireless communication systems using 5.8 GHz being deployed in the future. Anyone wishing to implement devices on a 5.8 GHz network could reference the data to predetermine communication behavior. In addition, the results will possibly justify the use of well-established Wi-Fi models or prove that unique model will need to be established.

Rationale for Methods and Equipment:

Ideally, a path loss study of 5.8 GHz would use equipment that is defined by hardware and not software. Specifically, a wave form generator equipped with an oscillator that could generate a 5.8 GHz would be needed. On the receiving end, a power spectrum analyzer rated up to at least 6 GHz would be used. Unfortunately, equipment rated for this specification are extremely expensive and not available, which is the reason SDRs are used instead. The SDRs will be limited in signal power production and signal detection accuracy. However, they will still be able to provide measurements suitable for an undergraduate research project.

The experiments use two of Ettus Research’s USRP N210 transceivers. The two SDRs are professional grade and versatile. The devices primarily serve as an analogue to digital converter with a high sampling rate. The N210’s valuable feature is its ability to utilize modular daughter boards and antennas. The CBX-40 1200-6000 MHz daughter board provides the mixing and filtering needed for the experiment. In addition, the N210 will accept any python or C+ code.

GNURadio will be the program used to provide control code to the SDRs. It is a free and open platform programing environment with plenty of online support. In fact, the N210 was designed to be used with GNURadio. The environment wraps python code into graphical user interfaces (GUIs) to build python code. In addition, it provides tools for building GUIs to display outputs and control program variables. The graphical interface is intuitive and does not require specific programing experience.

The first experiment will be to predict and measure path loss through free space. The Friis Transmission equation should predict the path loss within a small margin of error. While free space implies an infinite vacuum, the experiment will occur in a large, octagon-shaped room. This environment will contribute to error, but the error should remain relatively constant when measured in close proximity. The measured free space will also be centered in the room to best accommodate reflection and other distortions. The first experiment provides a proof of concept and measurements that can be used in the second experiment. Base line powers for ambient noise can also be recorded during this scenario.

The second experiment provides a more applied scenario. Path loss will be measured as the 5.8GHz propagates through open air, a wall, and then air again. The Partition Dependent model will be used to derive theoretical measurements for comparison. It is this experiment where the power limitations of the SDRs will have impact. There will be uncertainty in the accuracy of the measured received power given the constraint on power output of the N210. Precautions will be made to ensure the data collected is of the highest quality allowed by equipment limitation. Results from the first experiment will be used when calculation a wall's path loss in the analysis stage.

Theory:

First, a brief introduction into amplitude modulation is necessary for the full conceptualization of the experiment. Tone modulation will be used for this experiment. A single sinusoidal wave will be modulated, transmitted, received, and then demodulated. The tone will be a simple sinusoid with an arbitrary amplitude. The frequency is not important as long as it is half of the carrier frequency. It will be mixed or multiplied with a carrier signal. In this experiment, the carrier will be a sinusoid of same phase and have a frequency of 5.8 GHz. The result will be a dual sideband suppressed carrier signal (DSBSC). The transmitter then applies a gain to the signal if applicable. This DSBSC signal is what propagates and received at the receiver's antenna. To demodulate, the DSBSC signal is mixed with a signal identical to the original carrier signal. The mixing will create our desired message signal at the correct frequency and two at a very high frequency. The receiver then applies a low pass filter to only allow the low and recovered message signal to pass on for detection. In the case of the N210, a digital gain will be the final step if applied. Appendix A contains a mathematical and graphical explanation of DSBSC modulation. Understanding DSBSC modulation will help with determining appropriate variable values in the GNURadio code.

While the DSBSC signal is propagating to the receiver, it will be distorted. This experiment focuses on power attenuation that happens during the signal's travel. While the signal travels within line of sight of the receiver at equal elevation. The Friis Transmission equation will predict the amount of power delivered to the receiver. The equation states that the power received will lessen as distance away is increased and frequency is increased. See Appendix B for further explanation of the Friis Transmission equation (Bevelacqua). Power can be more easily analyzed by converting to a logarithmic scale. In terms of decibels, the path loss in free space can be predicted by:

$$L_{free-space} = 20log_{10}\left(\frac{4\pi d}{\lambda}\right)$$

With terms in a logarithmic scale, power gains and losses have a linear relationship. The linear relationship leads to the development of link budget. Link budget allows for the power received at the receiver to be the sum of all power added into the system along with attenuations subtracted from the system.

$$P_{Tx} + G_{Tx} - P_L + G_{Rx} = P_{Rx} \quad \text{(all values in decibels)}$$

The equation can be easily adjusted to be in terms of path loss.

$$P_{Tx}(known) + G_{Tx} + G_{Rx} - P_{Rx}(measured) = P_L$$

This equation will be used when analyzing data from the first experiment that will measure path loss due to free space (Pahlavan, p 46-50).

For the second experiment, path loss is measured when a wall is introduced as an obstruction the signal must path through. Any wave passing though matter will undergo an attenuation. Path Loss due to a wall will be constant and can be simply added to the equation that predicts path loss in decibels. The Partition Depended model is then used,

$$P_L(dB) = C + 20\log_{10}(d) + \sum n_i w_i \text{ (dB)}$$

where C accounts for the frequency and adjustment constant. The last term is simply the summation of losses caused by walls. The "n" terms represent the number of "w" type walls (Pahlavan, p 46-50).

Pre-Experiment:

The pre-experiment section introduces the N210 transceiver and GNURadio. This section will also explain the installation of GNURadio and its use with the N210. A brief description of how to set up the communication system will be detailed. Appendix H contains a supply list that should be considered before any set up of the experiment.

First, it was necessary to install two instances of GNURadio on the two separate laptops. The laptops used were two Apple MacBooks running OSX El Capitan. The installation and troubleshooting detailed is unique and varies depending on variables such as OS and software versions. First, a package management system was needed for the installation of GNURadio. In the Mac case, MacPorts was used. In addition, the latest version of XQuartz was needed to run GNURadio. Instructions on GNURadio's websites were followed. The process will be briefly summarized. MacPorts uses script commands that call the installation of packets needed for GNURadio. Using the commands listed on GNURadio's website, a script was run to install GNURadio. It was a large install with numerous packages and drivers. A few packages failed to install. When a package fails to install, the error logs would show the object that failed. The "sudo port install <name>" command was used to install the missing package. After troubleshooting a few failed downloads, the download was completed after an hour or two.

Once installed, GNURadio can be launched through the XQuartz's terminal. Using the script "GNURadio-companion", the program can be launched. The UHD GUI's was used to interact with the N210. It may not be apparent, but "sink" is a term used for something a signal is put into. Sinks were used for fast Fourier transform (FFT) spectrum analyzers and output to the transmitter. The receiver was accessed with a UHD source GUI although it may not seem intuitive. The GNURadio code used for the transmitter and receiver are shown and explained in

Appendix C. Appendix C also contains the variable values needed for the system to function properly.

Once the GNURadio environment was installed, the CBX-40 daughter board needed to be installed to the N210's motherboard. The casing of the N210 was removed by unscrewing four screws on its rear. The daughter boards are made to easily pop in and out of two pin slots. The WBX board was replaced with the CBX board. With the CBX in place, Tx/Rx connecting wires were screwed into the face plate of the device. The CBX board has labels to which wire is the receiver or transmitter. When the casing was restored, the connecting wires were labelled either "Tx" or "Rx".

The N210 has three ports on its face that will be used. First, power can be supplied to the device via DC input shown as labeled 1 of Figure D-1 in Appendix D. Using the same figure, the Ethernet port, labeled 2, is used to connect the laptop and the N210 via an Ethernet cord. An Ethernet to Thunderbolt adapter was needed for the newer MacBook used in the study. Lastly, label 3 shows where the antenna can be connected depending on if the device is being used as the receiver or the transmitter.

On the initial compile and execution of the GNU code, an error was thrown stating that the UHD device cannot be found. This was the result of the laptop self-assigning a random IP address for the connection to the N210. To resolve, the Ettus Research website was referenced for the correct IP address for the N210. In the laptop's network settings, the IP address for the Ethernet connection to the N210 was manually entered. After resolving that issue, a wireless communication system was established and running. Essentially, an AM radio system is established using the DSBSC modulation scheme. Appendix E shows the block diagrams from the DSBSC system at both the transmitter and receiver.

There is a draw back when using a software defined radio in study that involves the measurement of power. The system is only able to measure power in relative decibels (dB). Thus, it was necessary to find a way to calibrate the system to obtain power in dBs with respect to miliwatts (dBm). The calibration process began with assuming on the maximum transmission power the N210 is capable of at 5.8 GHz. This value was determined by referencing performance data off the Ettus Research website. The website states that between 3GHz and 6GHz, a maximum transmission power should be between 12 and 22 dBm. Note, 12 dBm would be expected at 6 GHz and 22dBm at 3GHz. If the approximation is made that maximum power decrease with frequency is constant, then it can be assumed the maximum output power at 5.8GHz would be 12.6 dBm. When the gain on the transmitter is at max value, then the power raw power output is assumed to be 12.6 dBm. Next, a hardline connection was made between the transmitter and receiver with a 30 dB attenuator in between. Then, the power is read from the receiver's FFT GUI in relative dB. The 30 dB is accounted for by adding 30 to the value measured. The difference between the measured value plus 30 and 12.6 dBm is the bridge between relative power and absolute power. The difference can be made up by setting the receiver's gain to the value.

Next, two wooden stands were constructed to house the two N210s. The stands can be seen in Appendix I. The purpose of the stands is to hold N210s vertical so that their antennas are pointed upwards and not obstructed. They also house the equipment securely during the movements of the experiments. Floral foam blocks were carved to create an insert sleeve for the N210. The foam was prototyped and designed to allow for a snug fit while allowing ventilation of the N210. The insert sleeve was a precautionary measure to prevent damage to the transceivers.

The final pre-experiment step was to devise a solution to assure accurate distance between transmitter and receiver. The solution was to “lasso” the two antennas together with a piece of twine. At the end of each piece of twine would be two loops to lasso the antennas together. The pieces would be cut to specified lengths. This would allow the N210s to be moved and positioned feel, and the distance between them would be preserved when the twine was pulled taught. Twenty lassos were cut. They range from 0.25m to 5m with increments of 0.25m.

Experimental Methods:

The first experiment was designed to test the path loss due to free space. The actions detailed in the Pre-Experiment section were carried out before the experiment began. The receiver gain was set to 14 dB to calibrate the measurement system. First, a room was selected. The room chosen was the third-floor atrium found in Luter Hall. The room was chosen for it size and relatively symmetric layout. The room forms an octagon with two walls containing doors and one containing a small vestibule room. Appendix F can be referenced for a better understanding.

The goal of the experiment is measure the power received at the receiver when in line of sight of the transmitter. To optimize the capture of signal propagation through free space, the gap between the two devices needs to be centered in the room. By positioning the gap in the center, it limits the distortion caused by reflection. It is the twine lassos and a symmetric room was chosen. The experiment follows a simple procedure. First, the receiver and transmitter begin in the center of the room connected by the 0.25 meter lasso. After this measurement was taken, the next lasso would be attached and the devices pulled back equal distance till taught. The environment variable was the walls in which the receiver and transmitter were approaching. A trial would be completed after reaching the maximum lasso length of 5 meter. The next trail would begin again with 0.25 meter lasso but with two new different walls. Appendix F can be referenced for more clarity. Two walls make up a single environmental variable, therefore there were four unique trials.

After set up and calibration, the first trail was run. The first trial was between the large wall and the wall with the vestibule room. The receiver FFT display shows a live feed of the power spectrum along with a horizontal, green line. This line is an average of the peak power value under inspection. The number of samples used for the average was set to 30. By managing the number of samples, the display averages the incoming measurements. The display's precision is increased. Measurements were recorded in an Excel work sheet on the laptop controlling the receiver. The 20 sample points were collected for the first trial. Next, the receiver and transmitter were positioned between the walls with the double doors. Again, the same method was carried out. The remaining two trials placed the deceives between the intermediate walls.

The second experiment will add a wall between the transmitter and receiver. This wall divides two electrical engineering labs that are adjacent to one another. The wall reflects a typical partition wall used in Luter Hall. The receiver and transmitter were placed in line on either side of the wall. To have the receiver and transmitter in line with one another, an origin or starting point needed to be established in both rooms. This point was established by measuring five meters into the room from the wall that connects to the hallway. The five meters would mark the same point in either room. Next, new lassos were made from the ones used in the previous experiment. They were doubled up on themselves to be cut in two equal halves. One of the halves went to the transmitter side of the wall and the other to the receiver. The cut side of the strings were taped to wall at the marked origin. The receiver and transmitter were virtually tied together by the lasso with the addition of the wall. The effort is to follow the same method of ensuring accuracy of distance as used in the first experiment. As the receiver and transmitter were looped to the next size lasso, the distance was incremented the same as the first experiment, 0.25 meter. The thickness of the wall can be disregarded since its entire composition determines the amount of attenuation. Measurements from the first experiment can assumed for the path loss through free space.

An Excel sheet was used again to collect data for the second experiment. In similar fashion, the first column represents distance the receiver and transmitter are from each other. The only difference from experiment one will be that the column will start at 0.25 meters away and not 0 meters. The following eight columns were for the separate trials. A trial was one cycle through all the strings. A cycle ended with the use of both 2.5 meter. Appendix G shows a diagram to better explain experiment two. Each trial had a different starting point on the wall to account for a stud or electrical wiring. The receiver and transmitter were moved 0.25 meters from the origin with the start of a new trial.

Measurements were taken using the same method as the first experiment. Received power was read directly from the FFT display produced by GNURadio. The averaging function of the display was increased to 100. Upon initial inspection, the system was more sensitive and additional was needed for the receiver to collect data and average it. A second pair of hands was needed to speed up the process of moving each radio. Each position was measured for a total of 160 data points.

Data:

The purpose of this section is to present the raw measurements collected by the two experiments and comment on them. Path loss values will be calculated and shown; however, path loss models will be applied and compared in the following sections.

The First Experiment – Path Loss Through Free Space

Table 1 – Raw Power (dBm) Received Through Free Space

Distance (m)	Trial 1	Trial 2	Trial 3	Trial 4	Average
0.25	-19.78	-15.42	-17.6	-19.78	-18.145
0.5	-24.13	-21.96	-23.41	-24.13	-23.4075
0.75	-29.94	-25.59	-27.04	-27.04	-27.4025
1	-31.4	-27.04	-30.67	-29.22	-29.5825
1.25	-32.85	-28.49	-32.85	-32.12	-31.5775
1.5	-33.58	-31.4	-34.3	-33.58	-33.215
1.75	-35.75	-31.62	-33.58	-35.57	-34.13
2	-35.03	-32.12	-38.66	-36.48	-35.5725
2.25	-39.29	-33.58	-36.48	-37.21	-36.64
2.5	-36.48	-39.39	-33.58	-37.93	-36.845
2.75	-35.08	-37.73	-40.48	-37.93	-37.805
3	-38.66	-37.93	-38.66	-37.21	-38.115
3.25	-42.29	-39.93	-37.21	-40.11	-39.885
3.5	-45.2	-39.93	-40.11	-37.93	-40.7925
3.75	-41.56	-40.84	-48.1	-39.39	-42.4725
4	-40.11	-37.93	-42.29	-40.11	-40.11
4.25	-43.74	-35.03	-46.65	-39.39	-41.2025
4.5	-41.56	-40.11	-46.65	-42.29	-42.6525
4.75	-43.02	-42.29	-44.47	-43.74	-43.38
5	-39.9	-37.93	-41.56	-48.83	-42.055

Table one shows the raw measurements taken for the first experiment. An average column has been included. All powers shown are measured in dBms.

Figure 1

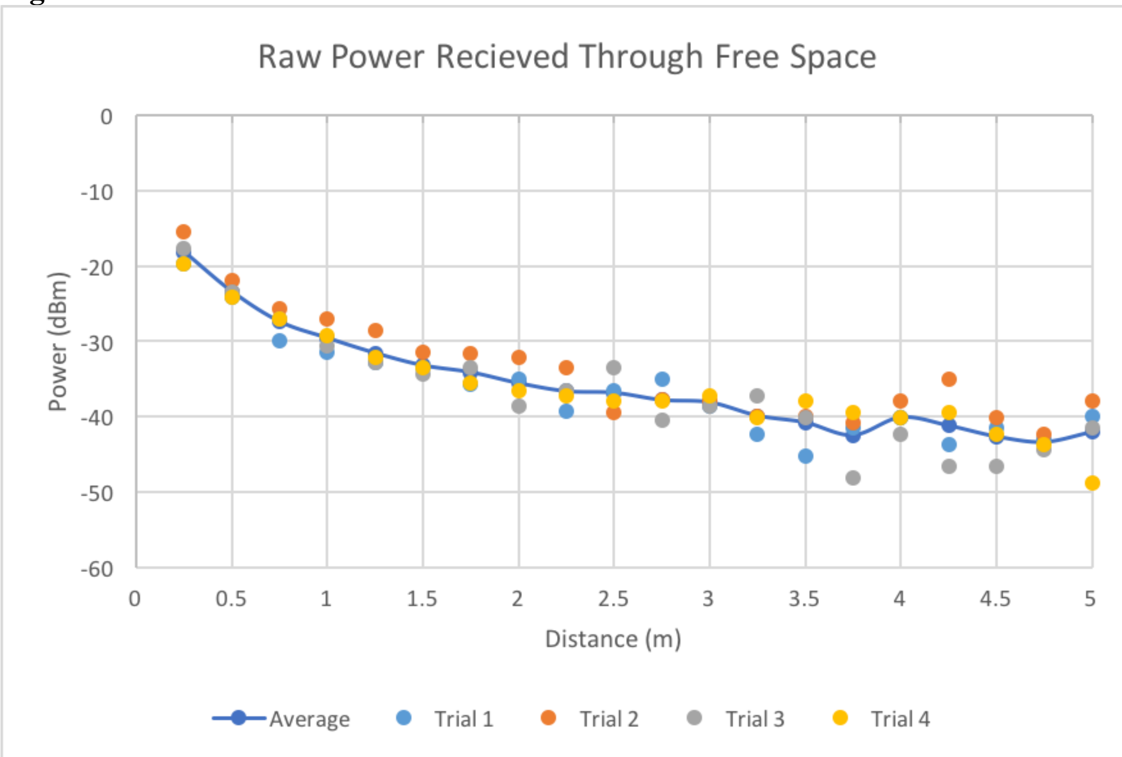

Figure 1 is the graphical representation of the data in Table 1. A connecting line was used in the Average data set to highlight the general trend of the data.

Table 2 – Calculated Path Loss Through Free Space

Distance (m)	Calculated Path Loss
0.25	30.745
0.5	36.0075
0.75	40.0025
1	42.1825
1.25	44.1775
1.5	45.815
1.75	46.73
2	48.1725
2.25	49.24
2.5	49.445
2.75	50.405
3	50.715
3.25	52.485
3.5	53.3925
3.75	55.0725
4	52.71
4.25	53.8025
4.5	55.2525
4.75	55.98
5	54.655

Figure 2

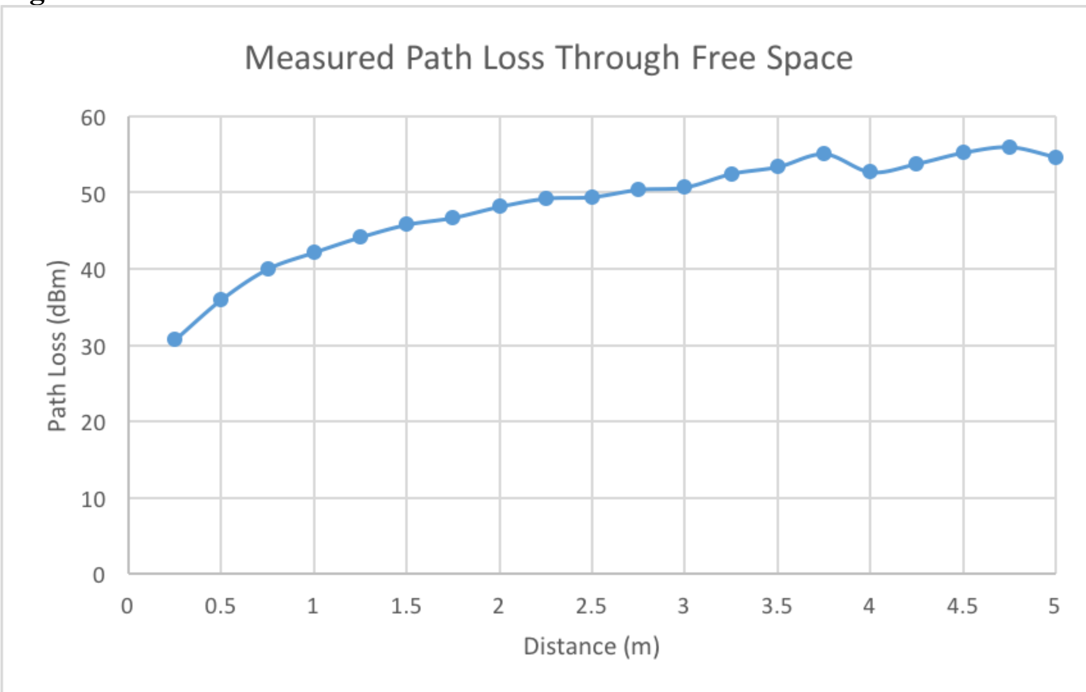

Figure 2 shows the graphical representation of Table 2.

The Second Experiment – Path Loss Through a Wall

Table 3 – Raw Power (dBm) Received Through Wall

Distance (m)	Trial 1	Trial 2	Trial 3	Trial 4	Trial 5	Trial 6	Trial 7	Trial 8	AVG
0.25	-54.64	-58.27	-56.82	-56.09	-55.36	-54.64	-52.94	-55.29	-55.50625
0.5	-50.28	-60.45	-51.73	-52.46	-53.91	-61.9	-57.65	-58.24	-55.8275
0.75	-52.46	-58.99	-52.46	-57.54	-50.28	-55.36	-52.35	-57.65	-54.63625
1	-50.28	-61.17	-49.55	-56.09	-50.28	-56.09	-61.19	-54.71	-54.92
1.25	-50.28	-62.63	-52.46	-53.91	-62.28	-71.34	-54.12	-49.4	-57.0525
1.5	-59.72	-53.18	-56.09	-60.45	-61.9	-53.18	-55.88	-51.17	-56.44625
1.75	-60.45	-55.36	-55.35	-68.44	-52.46	-53.91	-51.76	-61.19	-57.365
2	-62.63	-52.46	-53.91	-60.45	-53.91	-55.36	-53.53	-61.78	-56.75375
2.25	-63.35	-57.54	-52.46	-57.54	-51.73	-56.82	-49.4	-54.12	-55.37
2.5	-47.37	-55.36	-51.01	-58.27	-56.09	-56.82	-52.35	-55.29	-54.07
2.75	-56.82	-58.27	-55.36	-51.01	-61.17	-52.46	-52.94	-53.53	-55.195
3	-56.09	-54.46	-56.09	-53.91	-58.99	-61.9	-63.54	-60.6	-58.1975
3.25	-48.83	-56.82	-61.17	-57.54	-51.73	-51.73	-58.83	-65.31	-56.495
3.5	-62.63	-61.17	-54.64	-62.63	-63.35	-53.18	-53.91	-59.42	-58.86625
3.75	-54.64	-54.64	-61.17	-61.17	-54.64	-58.27	-59.72	-54.71	-57.37
4	-58.27	-57.54	-64.08	-55.36	-62.63	-71.42	-56.09	-52.35	-59.7175
4.25	-52.46	-62.63	-57.54	-53.18	-56.09	-50.28	-63.46	-62.37	-57.25125
4.5	-53.91	-57.54	-58.99	-58.27	-64.08	-62.63	-54.64	-52.94	-57.875
4.75	-53.18	-59.72	-56.82	-56.09	-61.17	-66.26	-56.36	-55.88	-58.185
5	-60.45	-60.45	-58.99	-51.01	-66.53	-52.46	-56.09	-60.01	-58.24875

Table one shows the raw measurements taken for the second experiment. An average column has been included. All powers shown are measured in dBms.

Figure 3

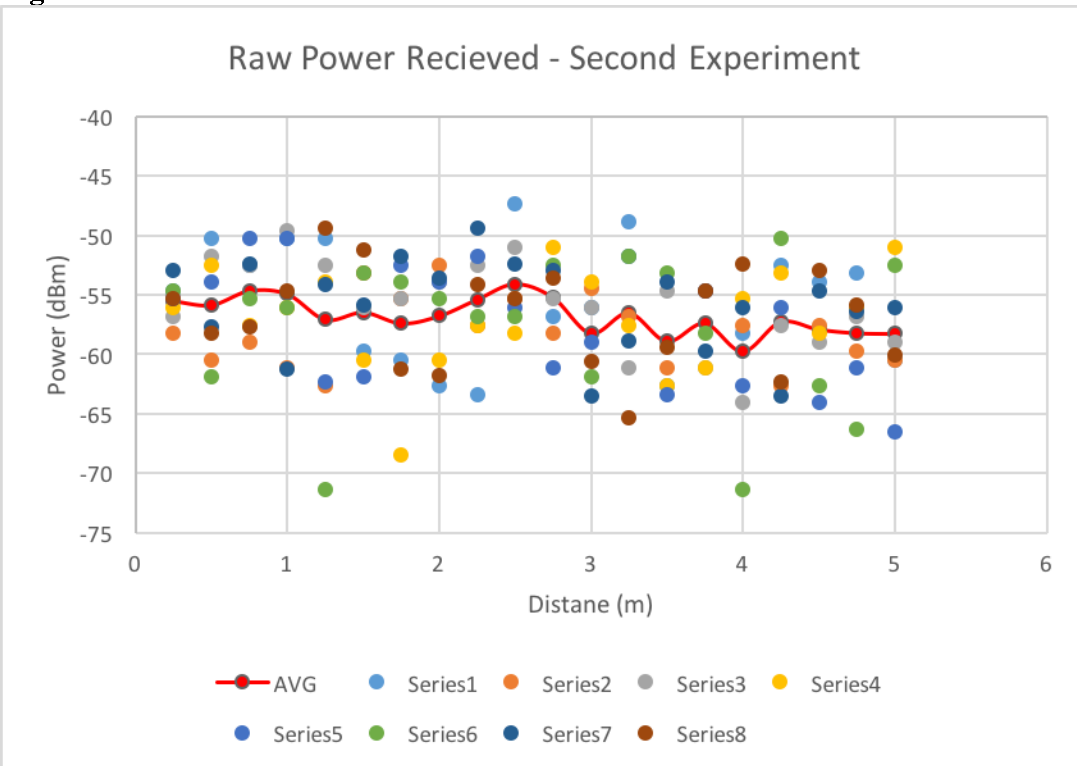

Figure 3 shows the graphical representation of Table 3. The key take away from the data spread is an oscillating trend in all data sets. It is apparent in the red line denoting the average.

Table 4 – Calculated Path Loss Through Wall

Distance (m)	Trial 1	Trial 2	Trial 3	Trial 4	Trial 5	Trial 6	Trial 7	Trial 8	AVG
0.25	36.495	40.125	38.675	37.945	37.215	36.495	34.795	37.145	37.36125
0.5	26.8725	37.0425	28.3225	29.0525	30.5025	38.4925	34.2425	34.8325	32.42
0.75	25.0575	31.5875	25.0575	30.1375	22.8775	27.9575	24.9475	30.2475	27.23375
1	20.6975	31.5875	19.9675	26.5075	20.6975	26.5075	31.6075	25.1275	25.3375
1.25	18.7025	31.0525	20.8825	22.3325	30.7025	39.7625	22.5425	17.8225	25.475
1.5	26.505	19.965	22.875	27.235	28.685	19.965	22.665	17.955	23.23125
1.75	26.32	21.23	21.22	34.31	18.33	19.78	17.63	27.06	23.235
2	27.0575	16.8875	18.3375	24.8775	18.3375	19.7875	17.9575	26.2075	21.18125
2.25	26.71	20.9	15.82	20.9	15.09	20.18	12.76	17.48	18.73
2.5	10.525	18.515	14.165	21.425	19.245	19.975	15.505	18.445	17.225
2.75	19.015	20.465	17.555	13.205	23.365	14.655	15.135	15.725	17.39
3	17.975	16.345	17.975	15.795	20.875	23.785	25.425	22.485	20.0825
3.25	8.945	16.935	21.285	17.655	11.845	11.845	18.945	25.425	16.61
3.5	21.8375	20.3775	13.8475	21.8375	22.5575	12.3875	13.1175	18.6275	18.07375
3.75	12.1675	12.1675	18.6975	18.6975	12.1675	15.7975	17.2475	12.2375	14.8975
4	18.16	17.43	23.97	15.25	22.52	31.31	15.98	12.24	19.6075
4.25	11.2575	21.4275	16.3375	11.9775	14.8875	9.0775	22.2575	21.1675	16.04875
4.5	11.2575	14.8875	16.3375	15.6175	21.4275	19.9775	11.9875	10.2875	15.2225
4.75	9.8	16.34	13.44	12.71	17.79	22.88	12.98	12.5	14.805
5	18.395	18.395	16.935	8.955	24.475	10.405	14.035	17.955	16.19375

Path loss was calculated for each position. The average is included. Measured path loss through free space was used in deriving these values.

Figure 4

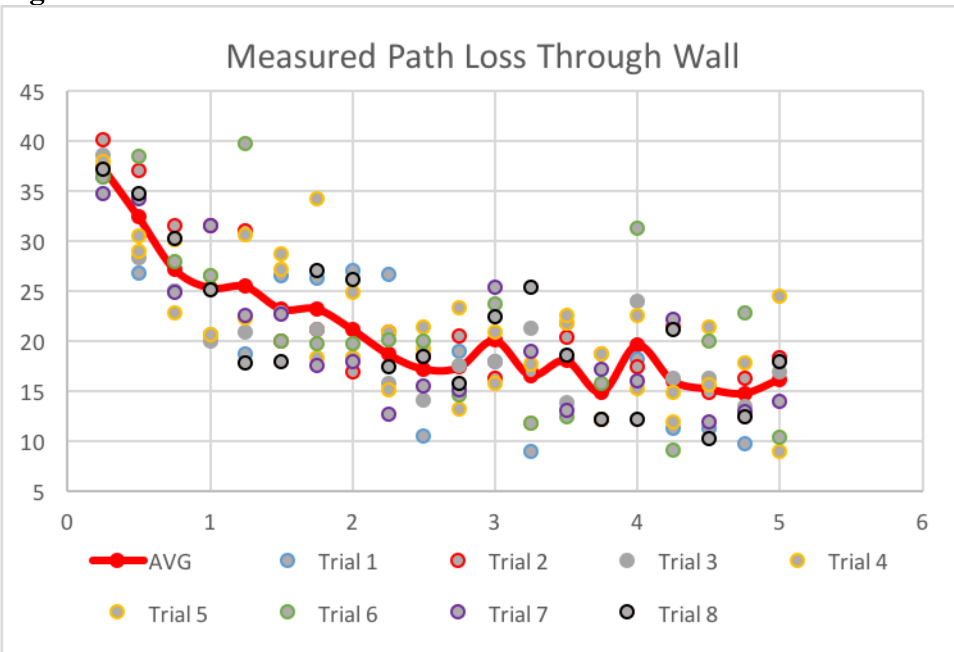

Figure 4 shows the data in Table 3. It may not be apparent yet, but the path loss seems to be opposite of what one may expect.

Data Analysis and Path Loss Models:

The First Experiment

Figure 5

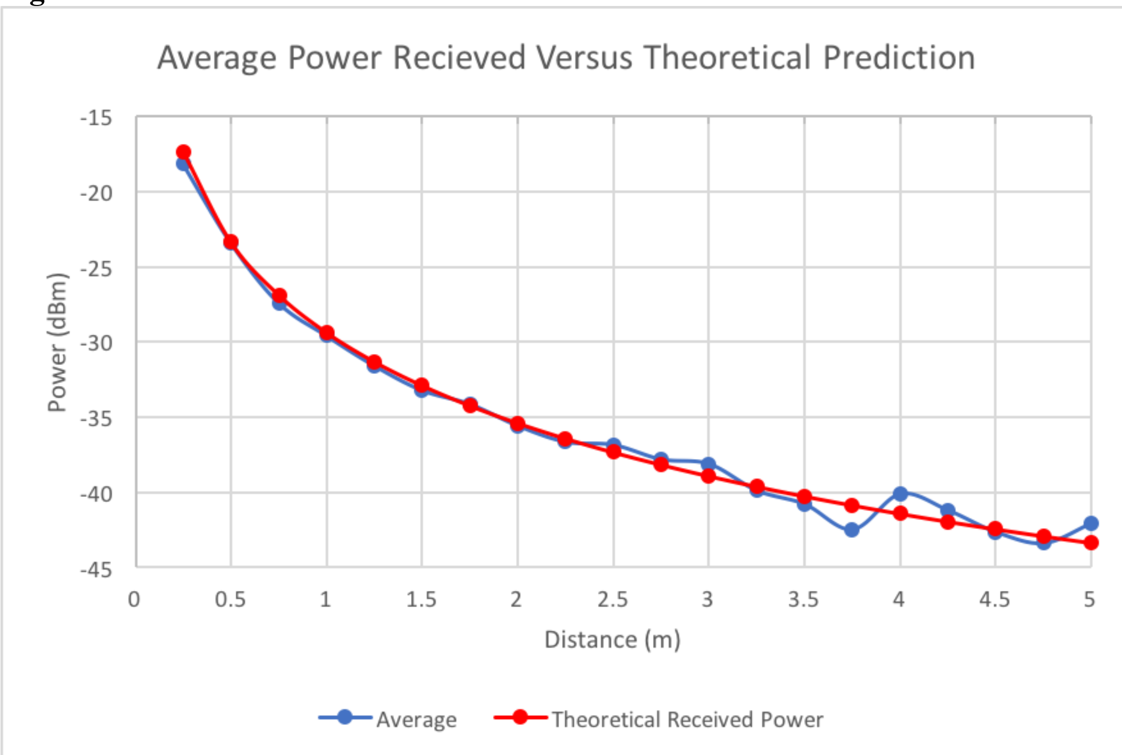

Figure 5 shows the average power received versus the expected power from the Friis Transmission equation. The Friis transmission equation almost completely matches the average of the measurements. Error arises as distance exceeds 3.5 meters. There error is expected. At that distance, the receiver is nearing the wall behind it making it more susceptible to interference from the wall. The octagon shape of the room may also be providing a satellite dish affect with reflection and multipath interference. When the distance is kept below 2.5 meters, the prediction is extremely accurate. Below this distance is also a truer representation of free space.

Figure 6

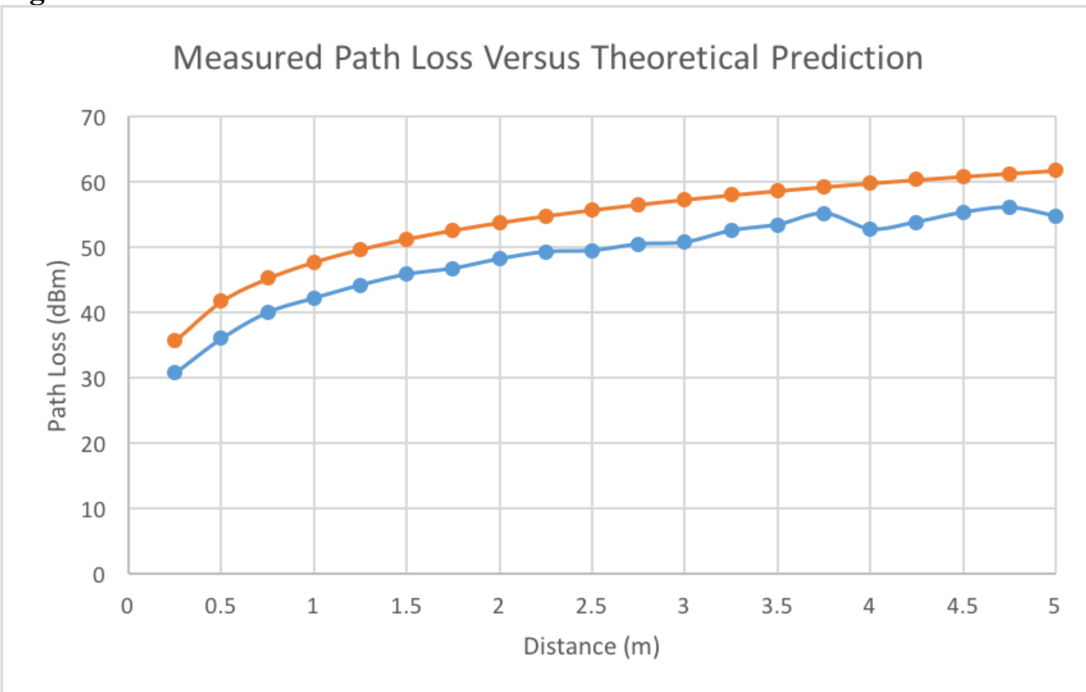

Figure 6 shows the calculated path loss through free space and the free space model derived from the Friss transmission Equation. At first glance, the model seems to predict the trend just with an offset. It is common for empirical constants be added to path loss models to adjust their fit. These constants account for power gains or losses in equipment which may not be able to accurately predict or correct. The next step was to apply a constant for the best fit.

Table 5 – Analysis of Path Loss Through Free Space Model

Distance (m)	Average	Calculated Path Loss	Theoretical Path Loss	Adjusted model	Percent error
0.25	-18.145	30.745	35.67736004	30.12236004	2.067035765
0.5	-23.4075	36.0075	41.69795996	36.14295996	0.374789331
0.75	-27.4025	40.0025	45.21978514	39.66478514	0.851422388
1	-29.5825	42.1825	47.71855987	42.16355987	0.044920611
1.25	-31.5775	44.1775	49.65676013	44.10176013	0.171738879
1.5	-33.215	45.815	51.24038505	45.68538505	0.283712061
1.75	-34.13	46.73	52.57932084	47.02432084	0.625890687
2	-35.5725	48.1725	53.73915978	48.18415978	0.024198377
2.25	-36.64	49.24	54.76221023	49.20721023	0.066636101
2.5	-36.845	49.445	55.67736004	50.12236004	1.351412911
2.75	-37.805	50.405	56.50521375	50.95021375	1.070091189
3	-38.115	50.715	57.26098497	51.70598497	1.916576904
3.25	-39.885	52.485	57.95622709	52.40122709	0.15986822
3.5	-40.7925	53.3925	58.59992076	53.04492076	0.655254522
3.75	-42.4725	55.0725	59.19918523	53.64418523	2.662571476
4	-40.11	52.71	59.7597597	54.2047597	2.757617055
4.25	-41.2025	53.8025	60.28633847	54.73133847	1.697087077
4.5	-42.6525	55.2525	60.78281015	55.22781015	0.044705472
4.75	-43.38	55.98	61.25243206	55.69743206	0.507326686
5	-42.055	54.655	61.69795996	56.14295996	2.650305504

Off Set
-5.555

Max Error	Avg Error	Std Dev
2.757617055	0.999158061	0.963474903

Table 5 shows a full analysis for the free space path loss model. The theoretical path loss model column shows the data used in Figure 6. The free space model was then adjusted with an offset -5.555. The percent error was calculated between the average and the adjusted model. Max error, average error and the deviation of the error was calculated. The offset was chosen to minimize the average error and standard deviation of the percent error data set.

Figure 7

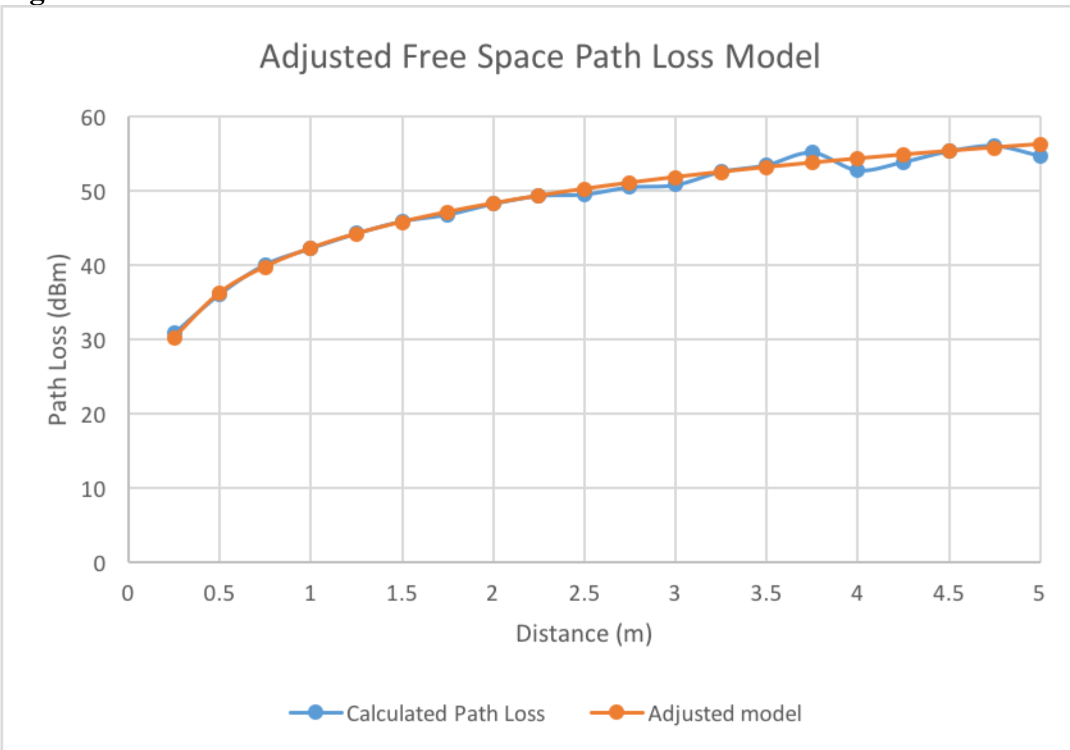

Figure 7 shows the fit of the adjusted model to the measured path loss due to free space. Graphically, the fit is near perfect. With an average error less than 1% and a max error of 2.7%, it can be asserted that the adjusted free space path loss model is valid.

<u>**The Second Experiment – Path Loss Through a Wall**</u>

Figure 8

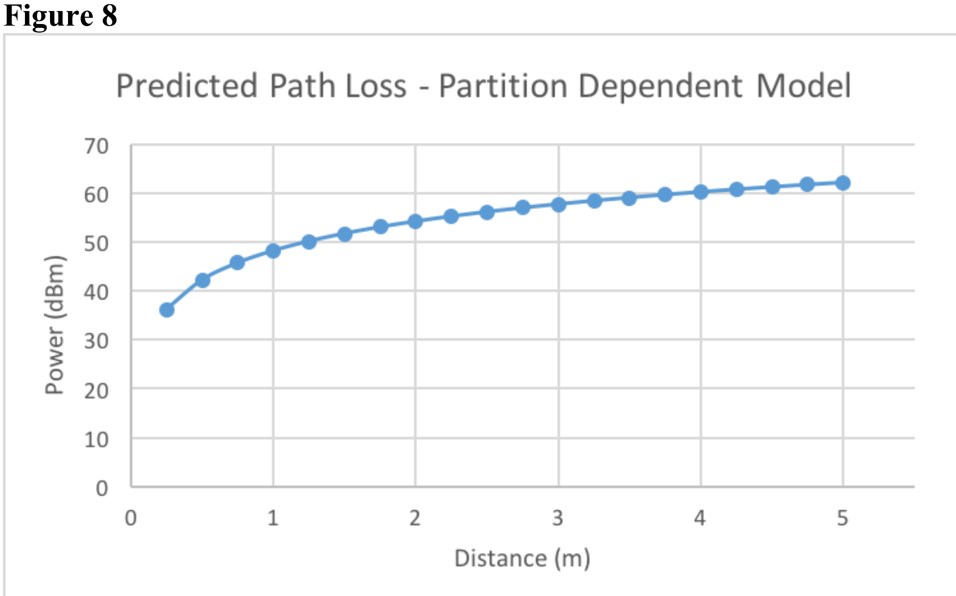

Figure 8 shows the Partition Dependent Model. This model is essentially a modification of the free space model with an offset. The model predicts the wall to contribute a constant power loss over the entire distance. This constant was deemed to be -6dB based on the results of the a experiment done at Harris Semiconductors. In referencing Figure 4, it is obvious this model does not correlate to the measured results. A new model must be devised. First, addition analysis of the measured results is needed.

Figure 9

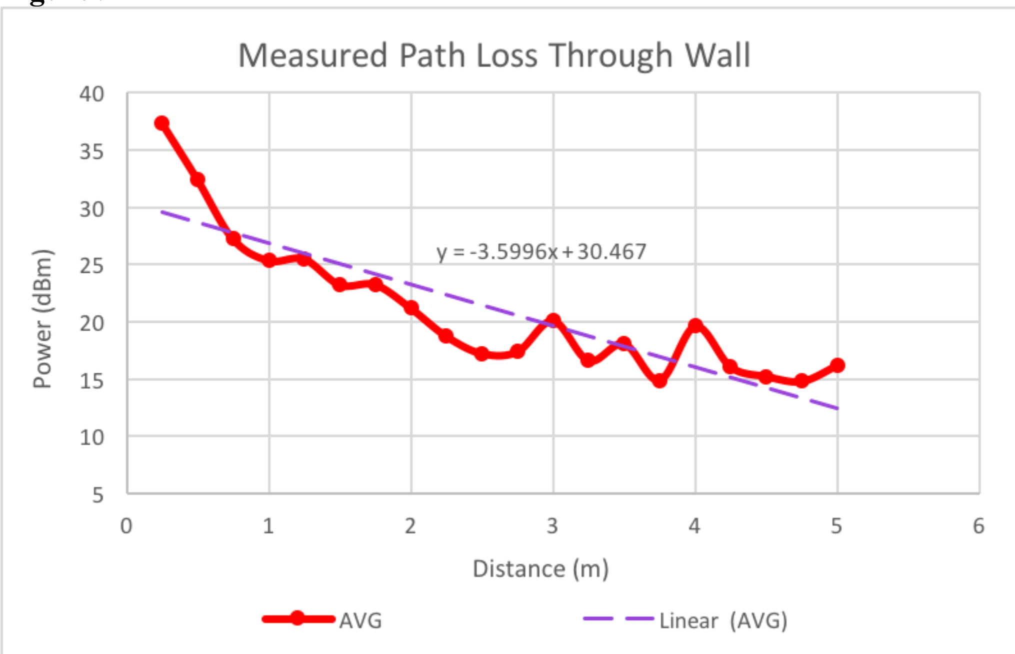

Figure 9 shows the average data set of the second experiment fit with a linear trend line. The new model will follow the typical equation set up as most path loss models dependent on distance:

$$L = (10 * n) \log_{10} d + C$$

n – loss exponent
C – off set which included and adjustment contestant and path loss due to free space.

A model based upon the average of the experiment data could be defined by solving for the two variables above. The linear fit was used as a starting point. The loss exponent was set to -3.5996 and C was set to 30. Note, C includes the other terms from the adjusted free space model. Those values had been pre-calculated and stored in the Excel sheet used. The offset of 30 referred to here is an additional empirical constant used to better fit the model. As in the first experiment, percent error will be used to compare the model to the measured results. Specifically, the average error, max error, and standard deviation of errors will be considered.

Table 6 – The Luter Model Analysis

Distance (m)	Luter Model	Measured Path Loss	Percent Error	
0.25	37.45357972	37.36125	0.246517755	*n*
0.5	32.3360698	32.42	0.259555979	-3.7
0.75	29.34251839	27.23375	7.1867328	
1	27.21855987	25.3375	6.91094562	Off Set (C)
1.25	25.57108965	25.475	0.375774562	-15
1.5	24.22500847	23.23125	4.102200702	
1.75	23.08691304	23.235	0.641432469	
2	22.10104994	21.18125	4.161792979	
2.25	21.23145706	18.73	11.78184359	
2.5	20.45357972	17.225	15.7849128	
2.75	19.74990408	17.39	11.94893943	
3	19.10749854	20.0825	5.102716386	
3.25	18.51654273	16.61	10.29642932	Max % Error
3.5	17.96940312	18.07375	0.58069198	15.7849128
3.75	17.46002832	14.8975	14.6765416	
4	16.98354002	19.6075	15.45001795	Average % Error
4.25	16.53594806	16.04875	2.946296509	6.468365766
4.5	16.11394714	15.2225	5.532146342	
4.75	15.71476851	14.805	5.789258093	StdDev of % Error
5	15.3360698	16.19375	5.59256846	5.225292446

It was decided to call this new model the Luter Model for the namesake of the location. The above table shows the values of Luter model when using a *n* value of -3.7 with an off set, C, of -15. These values were chosen for their ability to minimize the average percent error while not causing a spike in the max error or deviation. For example, it was possible to minimize the average error to 6.2%. That *n* value also caused the max error rise to over 20% and deviation to over 6. Thus, the two given values were deemed optimal when balancing all three attributes of the percent error data set.

Figure 10

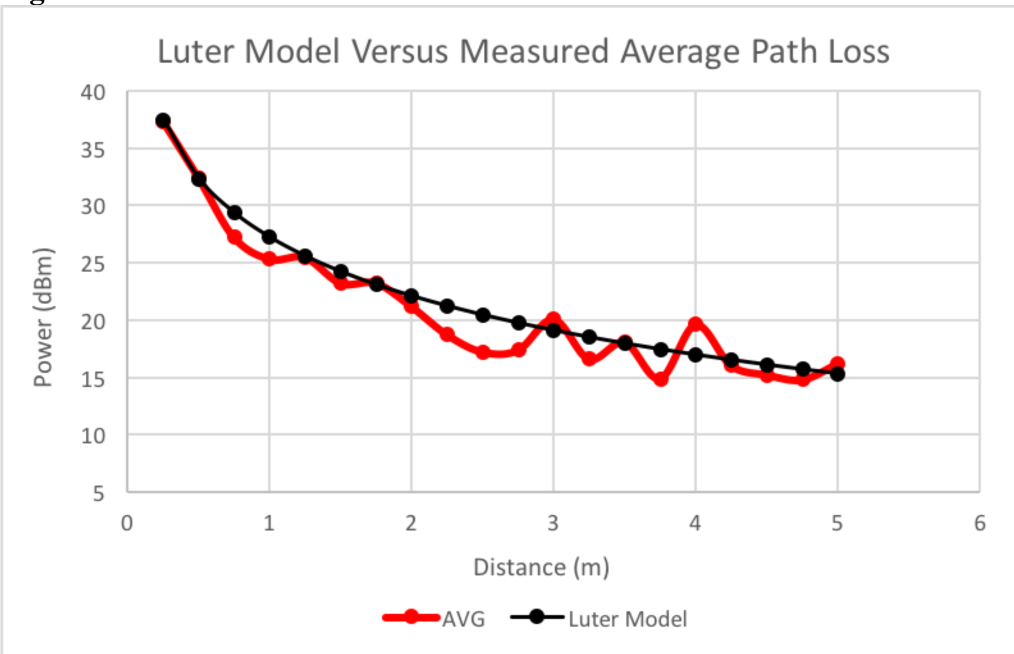

Figure 10 shows graphically how the Luter Model compares to the measured average path loss through a wall. The Luter Model will be formally presented in the following section. In addition, an explanation will be given for why the Partition Dependent model would not work.

Discussion and Conclusions:

First, the first experiment tested the use of the free space path loss model derived from the Friss Transmission Equation in Luter Hall. The free space model requires the transmitter and receiver to be within line of sigh of one another. Free space also requires the environment to be virtually obstruction free. Floors, ceilings, and walls are obstructions. But if the gap between the radios is centered in the room, the scenario can still be considered free space.

In this experiment, it was determined that the free space path loss model is valid and accurate. In reference to Figure 5, the Friss Transmission Equation was near perfect in predicting the raw received power at the receiver. Only when the radios came within proximity to the wall was there error is predicting the values. Which is expected, the hard surface is causing reflective interference. When calculating path loss and comparing to the free space path loss model, there was an initial off set. This off set was corrected with empirical constant that accounts for un measurable error within the receiver. With consideration to Figure7 and Table 5, it can be asserted that the adjusted free space path loss model is valid and accurate.

The adjusted free space model could be used in the future confidently when using a carrier frequency of 5.8 GHz. The results of the first experiment support any calculations or assertions made in the second experiment. The experiment was successful in both validation the model and provide a proof of concept for the second experiment. The adjusted free space path loss model for 5.8 GHz:

$$L_{free-space}(dB) = 20\log_{10}(d) + 20\log_{10}(5800MHz) - 27.55 - 5.555$$

Condensed:

$$L_{free-space}(dB) = 20\log_{10}(d) + 42.1636$$

The second experiment extended the first with the addition of a partition between the transmitter and receiver. This partition was a wall found between to electrical engineering labs in Luter Hall. It was selected because it best represents the standard partition wall one would find in the building. It would be the most common partition to encounter if one were implementing a communication system at 5.8 GHz. Initially, it was uncertain on how the signal having to propagate in and out of a wall would affect power. It was decided to attempt to use the Partition Dependent Model which assumes the wall causes a constant attenuation over all distances. The constant attenuation was selected from Harris semiconductors who performed a similar experiment just at 2.4 GHz.

A quick glance at Figure 8 and Figure 9 shows that the Partition Dependent Model is not applicable for 5.8 GHz in Luter Hall. The two trends have no correlation. In fact, the measured results show oscillating values as distance is increased. The overall trend could be described a power gain and not an attenuation, which go against all intuition. With the Partition Dependent Model discredited, the next step was to provide a working model based on the measured data.

It was decided to name the model after the building. The Luter Model was created and fitted to minimize the average percent error between the prediction and the average measured path loss. The Luter Model:

$$L_{wall}(dB) = -37\log_{10}(d) - 15 + L_{free-space}$$

This model accounts for the entire path loss included loss due to free space. It would be used as the attenuating term in a link budget calculation.

The obvious question was why was there a trend to gain power after distance was increased? Why was there oscillations in the data? After further inspection, it was determined that multipath interference was occurring. Once the signal had propagated through the wall, iterations of the signal had split and taken different paths to the receiver. The paths differ because the signals bounce off one or more hard surfaces (walls, floor, etc.) before reaching the receiver. The result is a phase shift between multiple signals and then adding together at the receiver. Depending on the phases, constructive or destructive interference occurs. As the receiver was being moved, the geometry of the paths was changing. Thus, explaining the oscillations in the measurements. There was not enough time allotted to study the periodicity of the individual data. However, visual inspection shows the progression of local max and mins has some sort of periodicity. The overall trend was still for a power gain or lack of loss.

The second experiment was successful in proving that Partition Dependent model was not valid. It was also able to determine that a model that including multipath interference is needed to correctly predict the propagation of signal through a wall. As promised, the Luter Model was created to provide predictions based on the measured data. The Luter Model has low error given the complexity of the probation. It is the same complexity that does not allow the Luter Model to be extended outside of its limited scenario. It confidently predicts the path loss between the two engineering labs only. Since multipath is a major factor, the geometry of the rooms plays a greater influence. The Luter Model is a great start, but further testing is needed to assert a model that would be universal between all the walls and rooms in Luter Hall.

<u>Appendix A:</u>

DSBSC Modulation

Negative frequency will be omitted to remain brief and on topic.

First, a message and carrier are defined as two cosine waves with arbitrary frequency; the carrier frequency is much higher that the message frequency.

$$message = \cos(f_m t) \text{ } in\ time\ domain$$

$$carrier = \cos(f_c t) \text{ } in\ time\ domain$$

Apply a Fourier Transform to both to view the signal in the frequency domain. Again, only positive frequency will be shown and graphed for brevity. In addition, the positive frequency component after the Fourier Transform will hold a relative 1 for power.

$$F[message] = \delta(f_m)$$

$$F[carrier] = \delta(f_c)$$

The delta function is an impulse in the frequency domain at the specifically frequency.

Graphically shown:

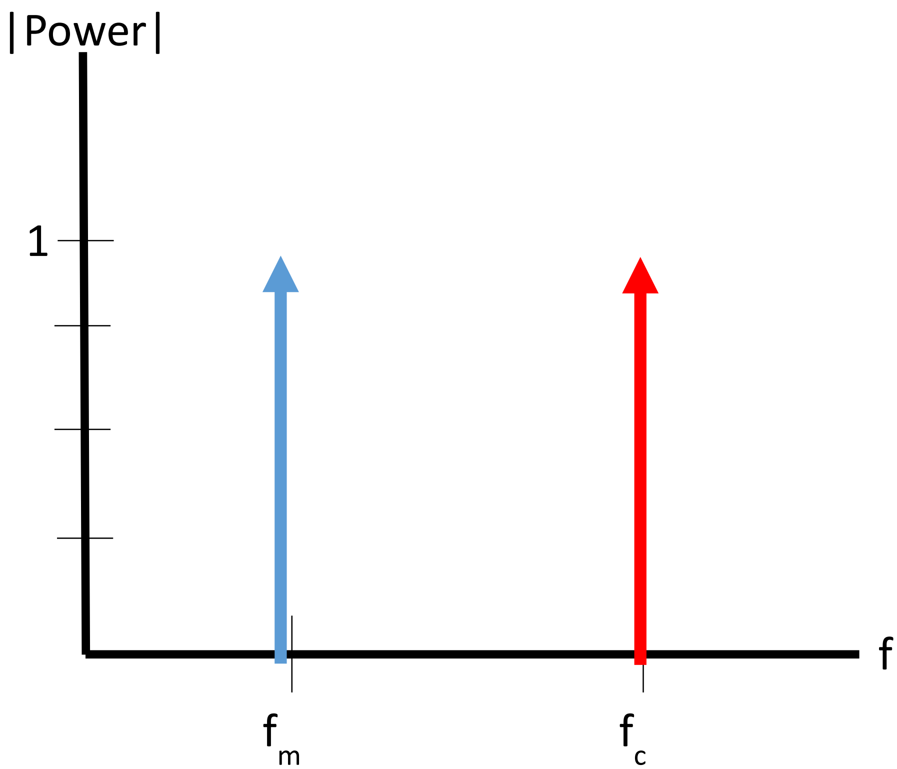

Mixing or multiplying the message and the carrier creates two impulses centered at the carrier frequency. The result is a DSBSC modulated signal that will be transmitted

$$message * carrier = \frac{1}{2}[\delta(f_c - f_m) + \delta(f_c + f_m)]$$

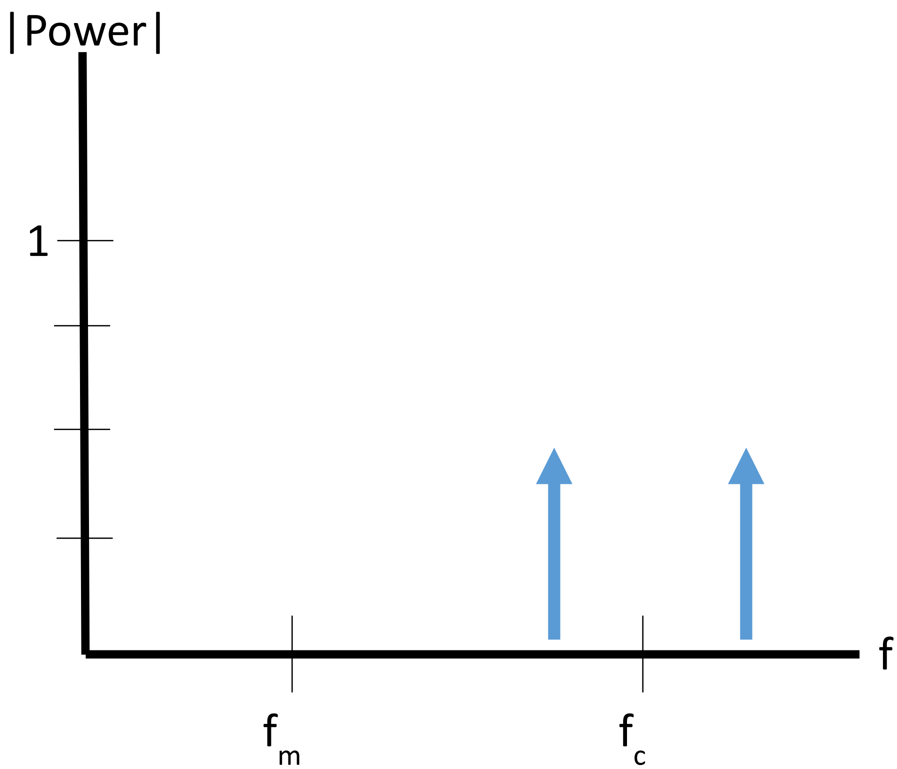

Once the signal is sent and received, the DSBSC signal is mixed with a wave identical to the original carrier frequency. The result is four impulses. Two will be at very high frequency. One will be pushed into negative frequency and the final signal will be at the original message frequency. A low pass filter will filter out the high frequencies to give the original message.

$$\frac{1}{4}[\delta[(f_c - f_m) - f_c] + \delta[(f_c + f_m) - f_c] + \delta[(f_c - f_m) + f_c] + \delta[(f_c + f_m) + f_c]]$$

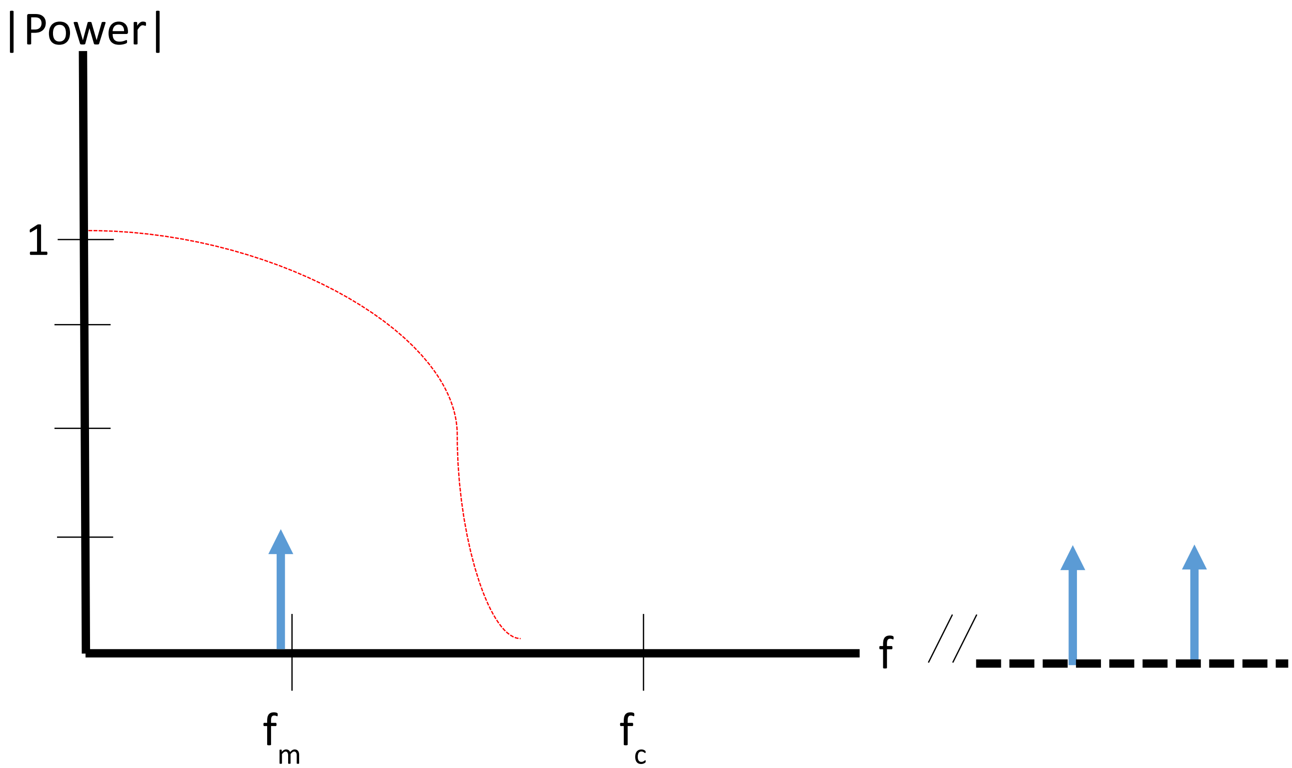

The impulse that is left makes up the message. The pulse will result in the original message at half power. Take the power loss and set it to a constant to represent the attenuation to account for any distortion and cost of modulation. Thus, DSBSC modulation and demodulation is complete with the original message with an attenuation.

$$After\ LPF = \frac{1}{4}[\delta[(f_c - f_m) - f_c] + \delta[(f_c + f_m) - f_c]$$

$$F^{-1}[\frac{1}{4}[\delta[(f_c - f_m) - f_c] + \delta[(f_c + f_m) - f_c]] = Acos(f_m)$$

$$Acos(f_m) = (attentuaion) * mesaage$$

Appendix B:

Friis Transmission Equation in watts:

$$P_{Rx} = \frac{P_{Tx}G_{Tx}G_{Rx}c^2}{(4\pi df)^2}\ (watts)$$

P_{tx} is the power output of the transmitter and is a known, constant value. G's constant gains of the receiver and transmitter. The other terms are constants, c being the speed of light. The equation on depends of distance and frequency. The result is increases in either will cause a growth in the denominator, meaning the power will be attenuated. With some hand waiving, path loss and be derived in decibels form this equation.

$$L_{free-space} = 20log_{10}(\frac{4\pi d}{\lambda})$$

Further manipulation can transform the equation into the radio engineering standard for path loss.

$$L_{free-space} = 20log_{10}(4\pi d) - 20log_{10}(\lambda)$$

Lambda is a wavelength and will become a constant.

$$L_{free-space} = C + 20log_{10}(4\pi d)$$

Now, path loss is depended on only the distance between the receiver and transmitter (Bevelacqua).

Appendix C:

Transmitter GNURadio Code

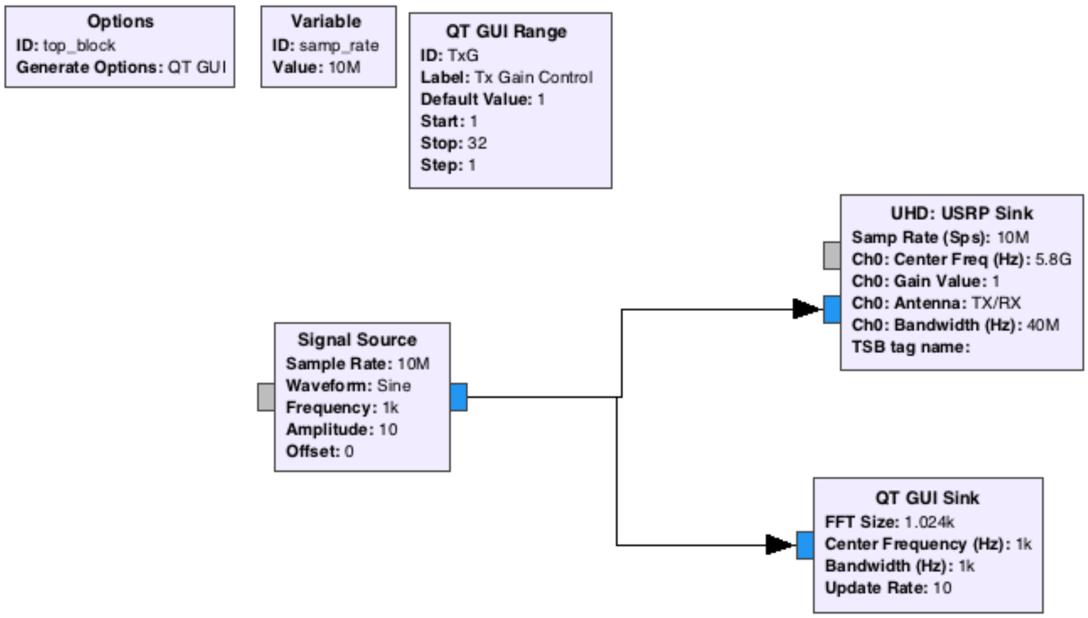

The GUIs above show the necessary variables and associate value to create the transmitter. The sample rate is set high to ensure resolution. Since data is not being stored, memory overflow is not a concern. The QT GUI Range widget named TxG adds a slider to the QT GUI Sink that allows the control of the transmitter's gain. It ranges from 1 to 32, 32.5 being the maximum gain of the CBX daughter board. The QT GUI Sink allows for monitoring of the message signal prior to transmission. The UHD: USRP Sink allows use of the N210 as a transmitter. The center frequency variable is how the mixing carrier signal is set. The bandwidth controls the BPF and should be set above 2000 Hz, since that is the bandwidth of the DSBSC signal.

Receiver GNURadio Code

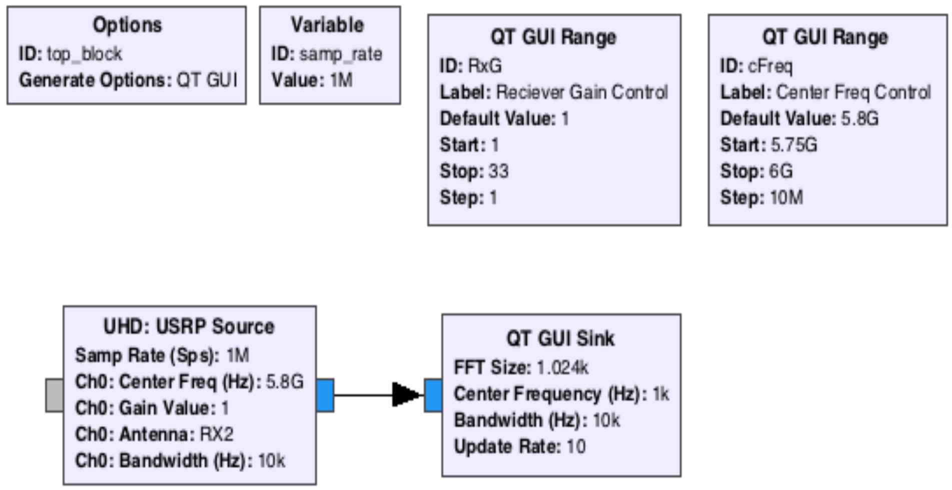

The GUIs above show the necessary variables and associate value to create the receiver. The sample rate is set to one million samples per second to ensure resolution. Despite the high sample rate, it should not cause memory over flow problems. The QT GUI Range widget named RxG adds a slider to the QT GUI Sink that allows the control of the receiver's gain. The other QT GUI Range widget named cFreq controls the value of the center frequency in the UHD: USRP Source. This variable control is to allow minor adjustments in demodulation if necessary. Again, the center frequency of the UHD: USRP Source is the mixing signal to demodulate the DSBSC signal. The band width is set to 10,000 Hz to allow only the capture of the true message signal. Finally, the signal is sent to a QT GUI Sink. The FFT display is centered around 1000 Hz to capture the message's power.

Appendix D:

Figure D-1

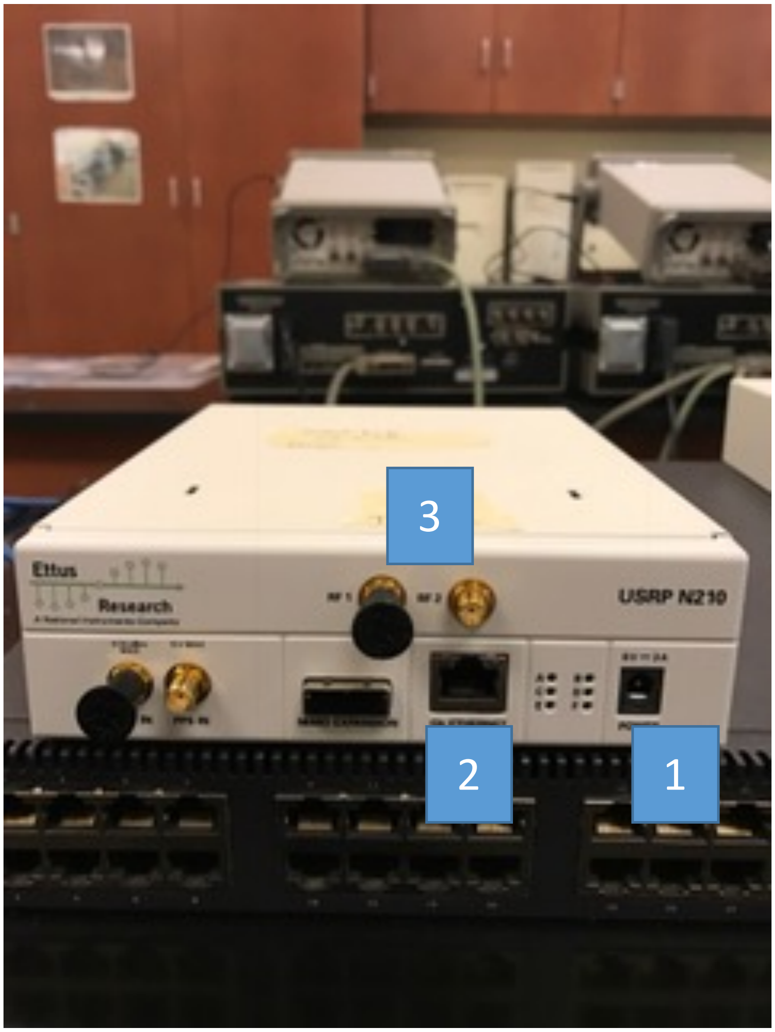

1- DC power in

2- Ethernet port

3- Tx/Rx antenna ports

Appendix E:

Block diagram for transmitter:

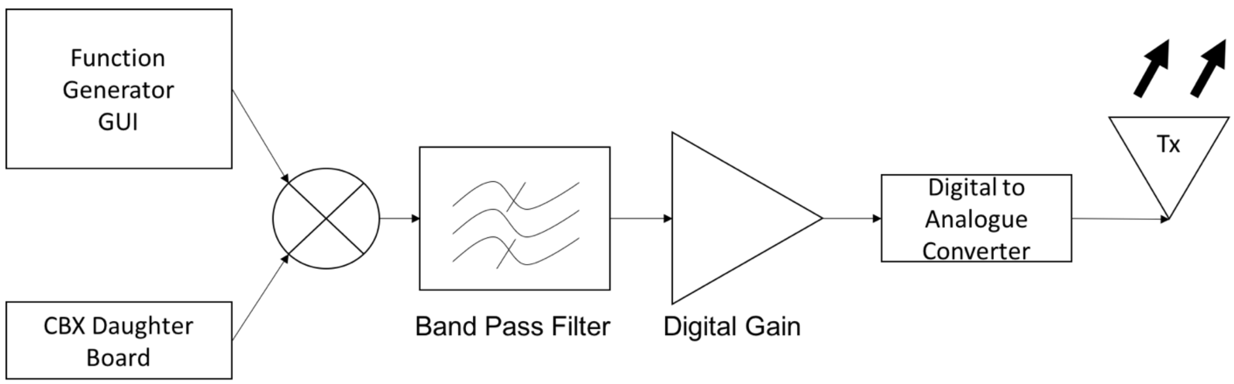

Block diagram for receiver:

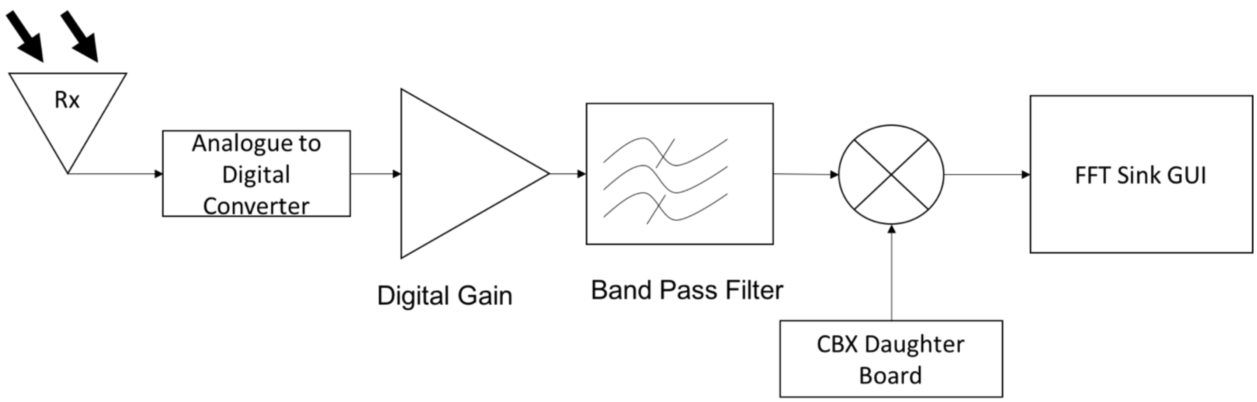

Appendix F:

Experiment one procedure diagram:

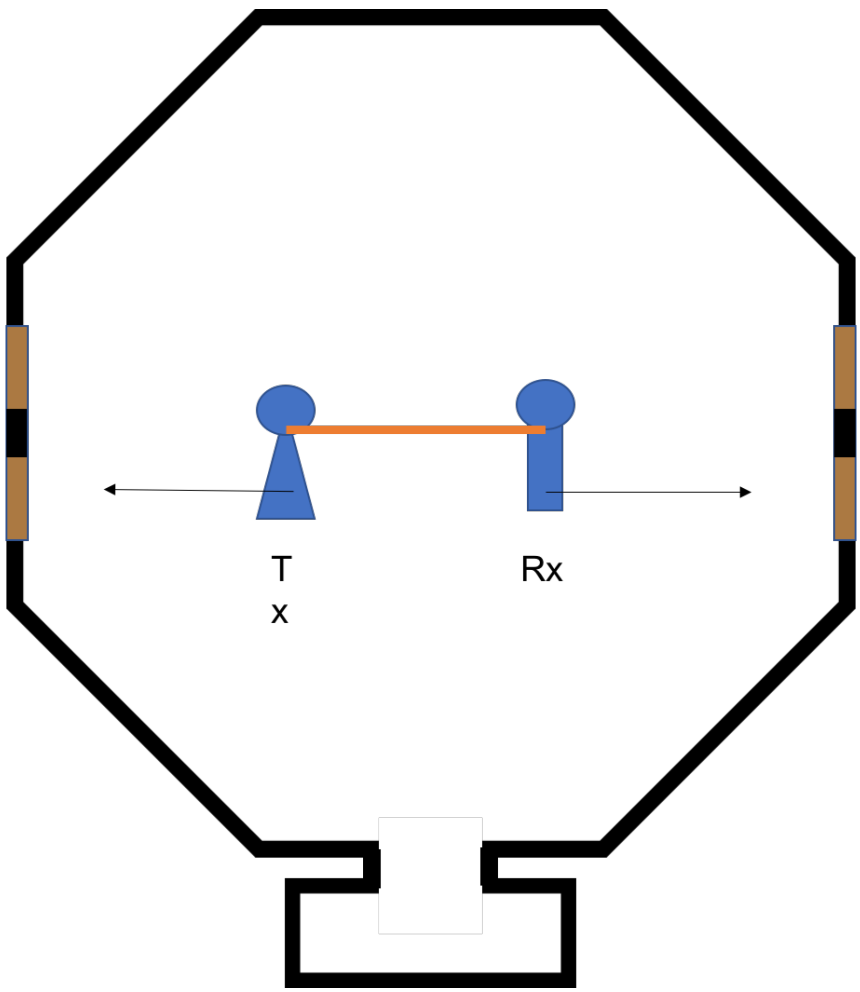

Appendix G:

Experiment two procedure diagram:

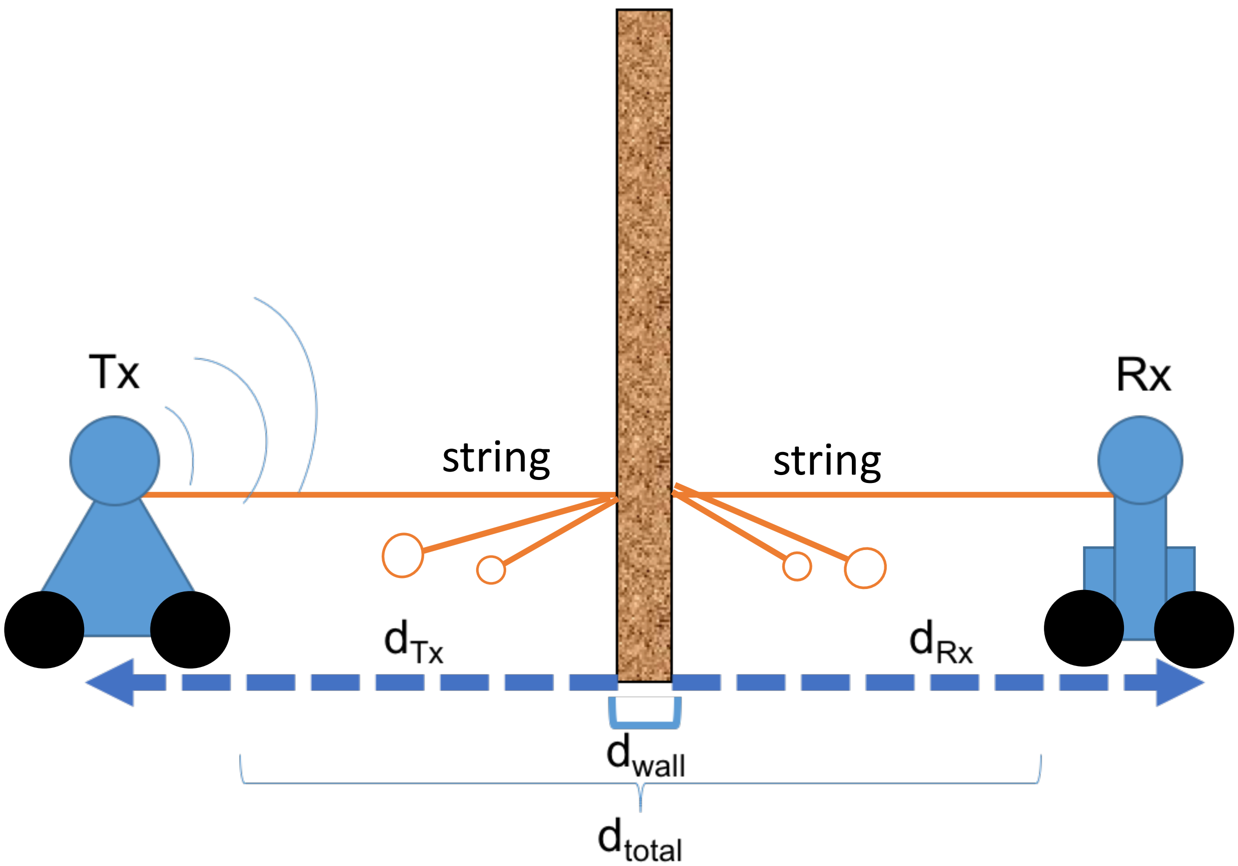

Appendix H:

Supply List

Quantity	Item	Description
2	USRP N210	Software defined radio transceiver
2	CBX 1200-6000 MHz Rx/Tx	RF Daughter board use to provide a high frequency carrier signal for mixing
2	Ettus Research VERT2450 antennas	A triband Tx/Rx antenna that can handle up to 6 GHz
1	Laptop	Need to produce Tx signal on transceiver
1	Laptop (highest available processing capability if not equal)	Used for collecting Rx measurements
2	GNURadio software	Downloaded to each laptop, free/open-source
2	Wooden stands with fitted foam sleeves	Used to hold N210s in upright position securely
1	Measuring tape (100ft/30m)	Needed for measuring string lengths
1	Masking tape	Used to mark distance measurements
1	100ft/30m roll of twine	Used for establishing distances with lasso system
1	Pair of Scissors	To cut string
1	Roll of masking tape	To label cut strings

Appendix I:

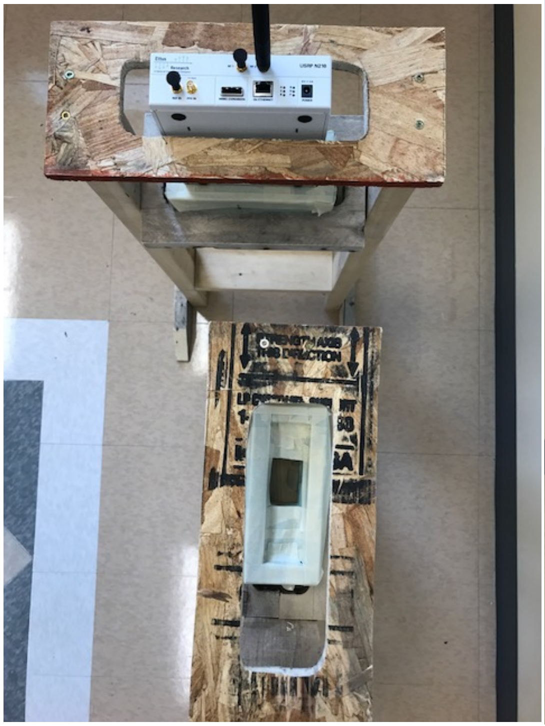

References

Bevelacqua, P. (n.d.). The Friis Equation. Retrieved September 19, 2016, from http://www.antenna-theory.com/basics/friis.php

Ettus Research. (n.d.). Retrieved September 21, 2016, from https://www.ettus.com/product/details/UN210-KIT

FCC Rules for Unlicensed Wireless Equipment operating in the ISM bands. (n.d.). Retrieved September 20, 2016, from http://www.afar.net/tutorials/fcc-rules

Pahlavan, K., & Krishnamurthy, P. (2002). Principles of wireless networks: A Unified Approach. Upper Saddle River, NJ: Prentice Hall PTR.

Schwengler, T., & Gilbert, M. (2000). Propagation models at 5.8 GHz-path loss and building penetration. RAWCON 2000. 2000 IEEE Radio and Wireless Conference (Cat. No.00EX404), 119-124. doi:10.1109/rawcon.2000.881870

Seidel, S., & Rappaport, T. (1992). 914 MHz path loss prediction models for indoor wireless communications in multifloored buildings. IEEE Transactions on Antennas and Propagation, 40(2), 207-217. doi:10.1109/8.127405